1979, *Astron. Astrophys. Suppl.* **38**, 251-263.

# RADIO CONTINUUM OBSERVATIONS OF THE NORTH POLAR SPUR AT 1420 MHz

Y. SOFUE*
Max-Planck-Institut für Radioastronomie, Bonn, Federal Republic of Germany
and
W. REICH
Radioastronomisches Institut der Universität Bonn, Federal Republic of Germany

Received October 11, 1978, revised March 6, 1979

Radio continuum observations at 1420 MHz of the North Polar Spur (NPS) were made with the 100-m telescope. Contour maps are presented for the region of $-6° \leq b \leq +20°$, $16° \leq l \leq 35°$ with a HPBW of 10′ in order to study the fine structure of the spur. The Narrow Neck region is nearly resolved and is shown to have many subridges. A sharp, thin ridge is found to extend from the main NPS ridge towards lower galactic latitudes, reaching as low as $b=2°$. A list of 250 radio sources stronger than 0.25 Jy in the observed region is presented. Source counts show that point sources at $b>6°$ are mostly extragalactic. Discussions are given of radio features of the NPS and some other interesting objects found in the mapped region.

*Key words:* Galactic radio Emission – North Polar Spur – Radio Sources

## 1. INTRODUCTION

The North Polar Spur is one of the most prominent features in the radio continuum background at high galactic latitudes ($b \gtrsim 10°$). It is part of a nonthermal radio ridge along a giant arc on the sky, Loop I, which has an apparent diameter of about 110°. It is not yet clear whether Loop I continues at negative latitudes. Many continuum observations of the background radio emission have covered this spur at various frequencies (see Berkhuijsen (1972) and references therein; Haslam *et al.* (1974)). The highest frequency used up till now was 820 MHz. In all these observations the main ridge of the NPS extends roughly from $(l, b) \cong (26°, 10°)$ towards the north, reaching as high as $b \cong 70°$. Because of insufficient resolution (HPBW > 0.5°), none of these observations resolved the narrowest part of the NPS.

In this paper we present new radio continuum data at 1420 MHz for the lower part of the NPS, i.e., $-6° \leq b \leq +20°$ and $16° \leq l \leq 35°$, with a resolution of 10′ (HPBW). The primary aim of the present observations is to study the fine structure of the NPS, in particular, of the Narrow Neck region, and to examine its further extension towards the galactic plane.

## 2. OBSERVATIONS AND REDUCTION

The observations were made in April 1977 and April 1978 using the 100-m telescope in Effelsberg of the Max-Planck-Institut für Radioastronomie. The allocated observing time was about 30 hours. The frequency was centered at 1420 MHz with a rejection filter against the neutral hydrogen line emission. The resulting bandwidth was 18 MHz. The major part of the observations was done in 1977 with a cooled parametric amplifier. The observations were done in the Dicke-switched mode using a helium cooled load. The system noise temperature was about 80 K. In 1978 additional measurements were done for the area $5.5° \leq b \leq 8.5°$, $23° \leq l \leq 30°$ and $-4° \leq b \leq 3°$, $l \leq 20°$ using a double channel uncooled parametric amplifier of 30 MHz bandwidth in the total power mode. The gain stability was good, but the system temperature

* A. von Humboldt-Fellow, present address: Department of Astrophysics, Nagoya University 464 Nagoya, Japan.

**Max-Planck-Gesellschaft zur Förderung der Wissenschaften E.V.**
**M.P.I. f. Radioastronomie, Bonn**
**Sonderdruck Nr 359, Ser. A**

for each channel was slightly higher than 80 K. Both equipments in 1977 and 1978 gave comparable results. The radio sources 3C345, 3C48 and 3C286 were used as flux and pointing calibrators. The HPBW of the antenna was roughly 9′.

Scans were made along constant galactic latitudes at an interval of 4′ at a scanning rate of 5° to 6° per minute. In order to derive the total intensity each area was scanned twice using orthogonal polarization angles. The integration time was 0.7 to 0.8 second effectively per data point. Reference scans were made along a few constant longitude lines for each field. For practical reasons the field between $b=5.5°$ and 8.5° taken in 1978 was scanned in latitude.

The resulting map was slightly smoothed to a HPBW of 10′ in order to increase the signal-to-noise ratio. Scanning effects were removed using a statistical method described in the Appendix. The data reduction was based on the programs of Neidhöfer *et al.* (1978) and Haslam (1974). The relatively strong sources, 4C+04.63 at $(l, b)=(32°45′, 10°37′)$ and PKS1735+35 at (27°29′, 17°55′), were used as secondary calibrators. Additional areas around these sources were mapped, smoothed to 10′ HPBW and compared with 3C286 whose flux was taken as 14.9 Jy (Genzel *et al.* 1976). The flux density of 4C+04.63 is determined to be $2.29\pm0.19$ Jy, and PKS1735+35 to be $1.53\pm0.09$ Jy. Some strong point sources near the galactic plane were also used for calibration; their flux densities were taken from Altenhoff *et al.* (1970). The aperture efficiency and the main beam efficiency were taken as 0.53 and 0.73, respectively (Internal Report of MPIfR, 1973). For our 10′ effective HPBW we derive the relation $T_b$ (in K)$=1.89$ S (in Jy) with an error of 10 percent, taking empirical values from our calibration sources.

The rms noise was determined in an area of $0.5°\times0.5°$ around $(l, b)=(34.3°, 16.7°)$. No sources or extended structure can be seen here. We found an rms noise in $T_b$ of 44 mK, slightly higher than the theoretical value of 30 mK. The larger value may be due to weather conditions, ground radiation effects, receiver gain instabilities and remaining interferences. The baselines of the maps were difficult to determine, because the elevation angle was mostly between 20° and 30°. We chose to adjust the baselines in such a way that the smoothed distribution of $T_b$ becomes consistent with the 408 MHz data (HPBW 37′) of Haslam *et al.* (1974) taken with the same telescope, assuming a temperature spectral index of $\beta=2.6$ (Wilson 1976), where $T_b\alpha\nu^{-\beta}$. A constant temperature correction was added to the whole region which sets the minimum temperature observed around $(l, b)=(27°, 19°)$ to zero. This adjustment holds for the area $b\geq8°$. Between $b=4°$ and $-4°$ the base levels were adjusted to the 1420 MHz data of Altenhoff *et al.* (1970). Necessarily our maps are not independent of these data used for the baseline adjustment, which influences the large-scale structure. However, the primary purpose of the present observations, to study fine structures in the NPS, is not affected.

## 3. CONTOUR MAPS

The results are shown in figures 1a-f, where the distribution of main beam total brightness temperature $T_b$ is presented in the form of contour maps. The minimum contour interval, 0.15 K, is 3-4 times the rms noise of the map. Outstanding features like the Galactic plane and the NPS are readily recognized on the map and are discussed in section 5.

Besides the fine structures associated with the NPS, we aim at examining its further extension towards the Galactic plane. The steep intensity gradient due to the Galactic emission, expecially below $b=6°$, makes it difficult to see such extended structures. To remove this difficulty we subtracted a smooth background from the map: the original map (figure 1) was convolved with a gaussian beam of HPBW $3°\times1°$ (in $l$ and $b$ directions) for the field above $b=6°$, and with a beam of $2°\times0.5°$ for the field below $b=6°$, yielding $\bar{T}_b^0$. Residual temperatures $\Delta T_b^0=T_b-\bar{T}_b^0$ were then subtracted from the original map only when $\Delta T_b^0$ is positive, yielding a map $T_b^1$. The map $T_b^1$ consists of two parts: where $\Delta T_b^0\leq0$, it is equal to the original map $T_b$; where $\Delta T_b^0>0$, it is replaced by the smoothed values $\bar{T}_b^0$. Hence the map $T_b^1$ is equal to the original

map $T_b$, except that small ridges and peaks are cut off at the level $\bar{T}_b^0$. The map $T_b^1$ was then again convolved with the same smoothing beam to get a smooth background $\bar{T}_b^1$.

Finally a residual distributions $\Delta T_b^1 = T_b - \bar{T}_b^1$ was obtained, which is shown in the form of a grey-scale plot with superposed contours in figure 2a. The figure exhibits the NPS structure more clearly than in figure 1, as well as many other features like point sources, extended galactic sources, and some other spur like features emerging from the Galactic plane. Figure 2b shows a contour plot of the smooth background $\bar{T}_b^1$ which has been subtracted from the original map.

## 4. POINT SOURCES

Many discrete sources are found in figure 1, and table 1 lists those with flux densities greater than 0.25 Jy. Salter's method (private communication) of finding sources and fitting them with a gaussian distribution was applied to the field: a flat background was assumed around each source. The peak positions and peak flux densities per beam of non-gaussian sources were found from our own program. In table 2 the integrated counts of sources per square degree $N(S_0)$ are given for $b>6°$ as function of limiting flux density $S_0$, and compared with counts from the literature (Maslowski 1973). For the point sources we find good agreement with the result of Maslowski at $b>20°$, who used the same HPBW as ours. We may therefore conclude that the point sources seen at $b>6°$ are mostly extragalactic. The NPS does not seem to contribute many point sources at the flux densities under consideration.

It is also of interest to see how the number density of sources varies with galactic latitude. Figure 3 shows the integrated source counts in several b-strips each 2° wide for the two cases of $S>0.25$ and 0.5 Jy. The density of sources including extended ones ($P$ and $E$) is highest at the Galactic plane, decreases steeply up to $b=6°$, and reaches a constant value at $b\geq 6°$. On the other hand the point source density does not seem to depend on galactic latitude. After subtraction of the constant component determined at $b\geq 6°$ the density of $P$ and $E$ sources is well fitted by a gaussian distribution around the Galactic plane with a half thickness of 2°. If we assume that the sources are distributed uniformly in a disk of 10 kpc radius, they are mostly within 400 pc from the Galactic plane.

## 5. COMMENTS ON OUTSTANDING FEATURES

### a) The North Polar Spur

Figures 1 and 2 reveal many structures associated with this spur. Below we discuss some remarkable features.

*i) NPS and its Narrow Neck:* In figure 1 the main ridge of the NPS runs from $(l, b)=(33°, 20°)$ down to (22°, 3°). The apparently narrowest part, so called Narrow Neck, is around $(l, b)=(29°, 13°)$ to (30°, 16°). Its typical width is about 0.8°. The spur structure in this region has been fully resolved except for point sources which we believe to be mostly extragalactic. We note that no significant narrowing of the ridge is seen in the Narrow Neck region, but the ridge becomes narrower at $(l, b)=(24°, 5°)$. Also remarkable is a splitting of the spur into several subridges, which are seen at $(l, b)=(33°, 20°)$ and (30°, 20°), at (31.5°, 16°) and (30.8°, 16°), and at (30°, 12°), (28.5°, 12°) and (27°, 11°).

*ii) Low-b extension of the NPS:* A remarkable finding of the present observations is a narrow radio ridge which extends from $(l, b)=(24°, 6°)$ to (22°, 3°). It seems to be an extension of the main ridge of the NPS, but makes a sharper angle (40°-45°) with the Galactic plane than the main ridge. Its thickness around $(l, b)=(23°, 4°)$ is about 0.3°. The ridge seems to split into two parts at $(l, b)=(22.5°, 3.6°)$: the southern branch leads toward a strong point source at $(l, b)=(21.0°, 2.0°)$, and the northern branch in the direction of the large HII region S49 (NGC6604) at (18.5°, 2°).

The point source on the southern branch has a flux density of $7.09 \pm 0.51$ Jy at 1420 MHz (table 1) and has a non-thermal spectral index of $\alpha = -0.56$ at $>400$ MHz, but a thermal spectral index of $\alpha = 0$ below 400 MHz. The HII region S49 and its connection to another large HII region S51 (M17) located at $(l, b) = (16.9°, 0.9°)$ are discussed in the next subsection. We find no direct extension of this ridge to lower latitudes or below the galactic plane.

We searched for possible optical counterparts to this low-$b$ extension of the NPS on the Palomar Sky Atlas and on the Hα Atlas of the Milky Way (Sivan 1974). But we failed to find any possible associated features either in emission or in absorption. We also examined distributions of starlight polarization in this field using data of Mathewson and Ford (1971), again failing to find any associated feature. The directions of polarization vectors (or magnetic field direction) are roughly perpendicular to the ridge in this field, and there is no significant change in polarization features across the ridge.

*iii) Ridge thickness:* In figure 4 we plot the thickness of the NPS against galactic latitude. The figure shows that the width increases linearly with latitude. We note that wide features ($\sim 3°$) might be difficult to detect at low latitude ($b \lesssim 6°$) because of the complex structures near the galactic plane. Figure 4 gives therefore the $b$-dependence of the mean *narrowest* width of the NPS.

### b) Some other remarkable features

*i) Two large HII regions, S49 and S51:* Two strong extended radio sources are seen at $(l, b) = (18.6°, 1.9°)$ and (16.9°, 0.9°), which are identified with the HII regions S51 and S49 (Sharpless 1959) (NGC6604 and 6611), respectively. Their temperature spectral indices are $\beta = 2.1$ for S51 and 2.2 for S49, which indicates that they are thermal sources. Both sources are located at a distance of 2.3 kpc (Minn and Greenberg 1973). In figure 1 we can recognize a radio bridge connecting these two sources, running from $(l, b) = (17.9°$, 1.8°) to (17.4°, 1.0°). The bridge might suggest a physical relation between these two HII regions, which agrees with the fact that they are located at the same distance from the sun. We remark that their optical appearance is very similar to the Orion Nebulae. S49 is associated with a dark nebula which resembles the Horse Head Nebula.

These two HII regions are located apparently on an extension of the low-b ridge of the NPS (northern branch). However, it is not clear whether there exists a relation between these HII regions and the NPS. If they were physically related, the distance of 2.3 kpc would disagree with current interpretations of the spur. The supernova-remnant hypothesis (e.g., Berkhuijsen 1971) postulates a distance of about 100 pc, and the galactic center explosion hypothesis (Sofue 1977) requires a distance of 8 kpc. Only the hypothesis that the NPS is due to a high-z non-thermal bank along a shocked inter-arm link between the local and Sagittarius arms (Sofue 1973) would be in agreement with this distance.

*ii) Chain of radio sources:* A peculiar chain of point sources is found centered at $(l, b) = (33.2°, 12.4°)$, where we count five sources (A-E in figure 5) within a thin strip of 5′ wide and 1.5° long. The most northern source A is 4C+06.64. We also find a point source F very near this chain at (32.5°, 12.5°). A radio bridge of about 0.3 K is seen, which extends from this chain towards the strong source G (4C+04.63) at $(l, b) = (32.8°, 10.6°)$. Both sources A and G have a non-thermal spectral index of $-0.8$ and $-1.0$, respectively. Figure 5 shows the contour map around this object, where the surrounding region was set to zero. Table 3 gives exact coordinates and flux densities of the sources in figure 5.

According to our source count in section 4, most of the point sources above $b = 6°$ are extragalactic. We may therefore conclude that the present association of sources is probably extragalactic. Possible interpretations are that this association is: a) a cluster of galaxies hidden by galactic dust because of its low galactic latitude (no cluster of galaxies is catalogued by Zwicky *et al.* (1960)); b) multiple radio sources associated with an active central galaxy at $(l, b) = (33.0°, 11.6°)$; c) a positional coincidence of unrelated sources. A deep careful optical survey as well as further radio observations with higher resolution is desirable.

## APPENDIX: CORRECTION FOR SCANNING EFFECTS

Due to ground radiation, weather conditions and receiver instabilities, base levels of individual scans are not necessarily constant. This appears on a final map as a scanning effect, or elongations of contour lines in the scan direction. To remove these effects, we applied the following method.

We assume that variations of the base levels along individual scans are independent of neighbouring scans. We also assume that the variation along each scan is a smooth function of distance along the scan direction. Suppose that the original map is composed of a mesh of $L \times M$ points and each grid at (i, j) has a data value $T_{ij}$ $(i=1, 2, \ldots L, j=1, 2, \ldots M)$. We smooth the map by a beam function with wider HPBW than the original (2-3 times the original HPBW) to get $\bar{T}_{ij}$, where $\bar{T}_{ij}$ is the data value at the $(i, j)$-th grid of the smoothed map. In the $\bar{T}_{ij}$, the scanning effect which appeared originally in $T_{ij}$ has already been smeared out, or "pressed out". Therefore a difference,

$$\Delta T_{ij} = T_{ij} - \bar{T}_{ij} \tag{1}$$

should include information only about the scanning effect and structures smaller than the smoothing HPBW.

Suppose now that the scanning was made in the i-direction. The difference $\Delta T_{ij}$ is then distributed at random around a smooth function which represents the scanning effect. Here we fit $\Delta T_{ij}$ with a polynomial of $n$-th order,

$$\Delta T_{ij} = \sum_{m=1}^{n} a_m^j \, i^m = s_{ij}. \tag{2}$$

The coefficients $a_m^j$ are determined by a least squares method. Finally $s_{ij}$ is subtracted from the original map to get a "true" distribution $T_{ij}^0$;

$$T_{ij}^0 = T_{ij} - s_{ij}. \tag{3}$$

Throughout this paper we used a gaussian beam of HPBW = 20′ (twice the original) as a smoothing function, and second order polynomials ($n=2$). To avoid the influence of strong radio sources, data points exceeding 10 σ were omitted from the least squares fitting, where σ is a standard deviation along each scan.

## ACKNOWLEDGEMENTS

The authors thank Dr. E.M. Berkhuijsen for valuable discussions and help with the observations. One of them (Y.S.) thanks Prof. O. Hachenberg for the opportunity to stay at the MPIfR, and the A. von Humboldt-Stiftung for a fellowship.

## REFERENCES

Altenhoff, W.J., Downes, D., Goad, L., Maxwell, A. and Rinehart, R.: 1970, *Astron. Astrophys. Suppl.* **1**, 319.
Berkhuijsen, E.M.: 1971, *Astron. Astrophys.* **14**, 359.
Berkhuijsen, E.M.: 1972, *Astron. Astrophys. Suppl.* **5**, 263.
Genzel, R., Pauliny-Toth, I.I. and Witzel, A.: 1976, *Technischer Bericht* Nr. 30, MPIfR.
Haslam, C.G.T.: 1974, *Astron. Astrophys. Suppl.* **15**, 333.
Haslam, C.G.T., Wilson, W.E., Graham, D.A. and Hunt, G.C.: 1974, *Astron. Astrophys. Suppl.* **13**, 359.
Mathewson, P.S. and Ford, V.L.: 1970, *Mem. Roy. Astron. Soc.* **74**, 139.
Maslowski, J.: 1973, *Astron. Astrophys.* **26**, 343.
Neidöfer, J., Wilson, W. and Haslam, C.G.T.: 1978, *Kleinheubacher Berichte*, Nr. 21, 215.
Sivan, J.P.: 1974, *Astron. Astrophys. Suppl.* **16**, 163.

Sofue, Y.: 1973, *Publ. Astron. Soc. Japan*, **25**, 207.
Sofue, Y.: 1977, *Astron. Astrophys.* **60**, 327
Wilson, W.: 1976, Ph. D. Thesis, University of Sydney.
Zwicky, F., Herzog, E. and Wild, P.: 1960, in *Catalogue of Galaxies and of Clusters of Galaxies*, Vol. 1, publ. Cal. Inst. Tech.

Y. Sofue

Max-Planck-Institut für Radioastronomie
Auf dem Hügel 69
D–53 Bonn 1 (Federal Republic of Germany)

W. Reich

Radioastronomisches Institut der
Universität Bonn
Auf dem Hügel 71
D–53 Bonn 1 (Federal Republic of Germany)

1979A&AS...38..251S

Table 1 List of 250 radio sources at 1420 MHz in the mapped region in figures 1a-f. There are given their galactic coordinates (*b, l*), peak flux densities ($S_p$), total flux densities (S), types (P: point; E: extended), spectral indices ($\alpha$), and identifications with sources in other catalogues (name, flux density, and frequency). See also notes to this table below.

| No. | b | l | $S_p$(Jy beam) | S(Jy) | Type | $\alpha$ | Identification Name | Flux (Jy) | Freq. (MHz) |
|---|---|---|---|---|---|---|---|---|---|
| 1 | -05°55!8 | 25°28!2 | .98± .12 | .98 | P | | OU-094 | 0.76 | 1415 |
| 2 | -05 43.0 | 26 08.1 | .26 .04 | .26 | P | | | | |
| 3 | -05 42.5 | 25 13.1 | .27 .18 | .27 | P | | | | |
| 4 | -05 42.9 | 20 29.9 | .22 .02 | .83 | E | | | | |
| 5 | -05 26.4 | 23 44.8 | .26 .05 | .26 | P | | | | |
| 6 | -05 14.1 | 21.54.44 | .16 .02 | .68 | E | | OU-179 | 0.46 | 1415 |
| 7 | -05 12.9 | 25 58.6 | .30 .03 | .30 | P | | | | |
| 8 | -05 05.3 | 22 58.1 | .61 .06 | .61 | P | | | | |
| 9 | -04 54.42 | 23 55.53 | .71 .05 | .71 | P | | | | |
| 10 | -04 45.0 | 20 21.7 | .20 .02 | .77 | E | | | | |
| 11 | -04 30.2 | 22 15.4 | .17 .04 | .29 | E | | | | |
| 12 | -04 26.9 | 24 29.8 | .32 .04 | .32 | P | | | | |
| 13 | -04 15.7 | 21 38.6 | .91 .09 | .91 | P | | | | |
| 14 | -04 15.5 | 22 36.2 | .33 .05 | .33 | P | | OU-175 | 0.68 | 1415 |
| 15 | -04 24.0 | 21 55.8 | .27 .03 | | E | | | | |
| 16 | -03 57.3 | 24 41.0 | .94 .09 | .94 | P | | OU-080 | 0.6 | 1415 |
| 17 | -03 46.0 | 25 39.7 | .21 .05 | .21 | P | | | | |
| 18 | -03 24.0 | 23 40.5 | .24 .05 | .24 | P | | OU-074 | 0.36 | 1415 |
| 19 | -03 30.3 | 18 22.0 | .34 .04 | .34 | P | | | | |
| 20 | -03 20.0 | 26 20.0 | .62 .08 | | E | | | | |
| 21 | -03 04.8 | 20 25.6 | .68 .07 | .68 | P | | ADG020.4-03.0 | 1.0 | 1414 |
| 22 | -03 03.1 | 18 22.7 | .45 .06 | .45 | P | | | | |
| 23 | -03 00.6 | 26 15.1 | .51 .05 | 1.92 | VE | | | | |
| 24 | -02 53.52 | 20 06.32 | .46 .05 | .70 | E | -.4 | CC 020-02.9. | 1.15 | 408 |
| 25 | -02 50.1 | 25 23.6 | .20 .03 | 1.19 | VE | | | | |
| 26 | -02 48.0 | 21 40.2 | .38 .05 | | E | | | | |
| 27 | -02 43.8 | 21 55.8 | .27 .03 | | E | | | | |
| 28 | -02 40.2 | 25 00.0 | .35 .04 | | E | | | | |
| 29 | -02 37.8 | 17 37.8 | .79 .10 | | E | | | | |
| 30 | -02 31.6 | 24 10.4 | .26 .03 | .62 | E | | | | |
| 31 | -02 31.5 | 16 52.5 | .73 .06 | 3.49 | E | | | | |
| 32 | -02 22.6 | 17 19.8 | 1.01 .11 | 2.66 | E | +0.3 | GD017.4-02.4 | 3.3 | 2700 |
| 33 | -02 15.3 | 18 29.5 | .28 .03 | 1.12 | P | | | | |
| 34 | -02 13.2 | 18 59.4 | .25 .07 | .25 | P | | | | |
| 35 | -02 12.0 | 25 07.8 | .57 .07 | | E | | | | |
| 36 | -01 59.5 | 19 44.5 | .52 .09 | .52 | P | | | | |
| 37 | -01 47.8 | 21 59.8 | .26 .04 | .26 | P | | | | |
| 38 | -01 42.52 | 24 52.52 | 1.43± .08 | 1.43 | P | -0.55 | CUL1840-07 | 7. | 80 |
| | | | | | | | | 4.8 | 160 |
| | | | | | | | BG1840-08 | 3.7 | 408 |
| | | | | | | | CC024-01.7 | 2.78 | 408 |
| | | | | | | | ADG024.9-01.7 | 1. | 1414 |
| | | | | | | | | 2. | 2695 |
| 39 | -01 40.9 | 20 21.0 | .37 .10 | .37 | P | | BG1831-12 | 2.4 | 408 |
| 40 | -01 34.0 | 21 06.1 | .35 .07 | .35 | P | -1.2 | CC021-01.6 | 1.73 | 408 |
| 41 | -01 31.8 | 23 16.2 | .45 .06 | .45 | E | | | | |
| 42 | -01 07.9 | 25 21.9 | .56 .07 | .56 | P | -0.7 | CC025-01.1 | 1.48 | 408 |
| 43 | -01 06.0 | 18 54.0 | 4.72 .58 | | E | | BG1825-13 | 2.6 | 408 |
| | | | | | | | ADG018.9-01. | 42. | 1414 |
| | | | | | | | | 27. | 2695 |
| | | | | | | | | 28. | 5000 |
| 44 | -01 05.1 | 16 46.8 | 2.93 .25 | 5.03 | E | -0.1 | CC016-01.2 | 1.18 | 408 |
| | | | | | | | ADG016.8-01. | 5. | 1414 |
| | | | | | | | | 4. | 2695 |
| | | | | | | | | 4. | 5000 |
| 45 | -00 58.7 | 20 56.3 | 1.12 .10 | 6.14 | E | | | | |
| 46 | -00 53.8 | 21 29.4 | 8.14 .33 | 8.14 | P | 0.0 | CUL1830-10.6 | 8. | 80 |
| | | | | | | | | 7.6 | 160 |
| | | | | | | | CC021.-00.9 | 4.98 | 408 |
| | | | | | | | ADG021.5-00. | 6. | 1414 |
| | | | | | | | | 7. | 2695 |
| | | | | | | | | 6. | 5000 |
| | | | | | | | GD021.5-00.9 | 6.7 | 2700 |
| 47 | -00 53.3 | 20 17.0 | 1.66 .17 | 2.93 | E | -0.1 | ADG020.3-00.8 | 3. | 1414 |
| | | | | | | | | 2. | 2695 |
| | | | | | | | GD020.2-00.9 | 3.7 | 2700 |
| 48 | -00 40.2 | 24 43.8 | 2.55 .31 | | E | | AJG084 | 12. | 408 |
| | | | | | | | ADG024.7-00.6 | 6. | 1414 |
| | | | | | | | | 3. | 2695 |
| 49 | -00 40.0 | 19 44.1 | 2.28 .22 | 4.82 | E | -0.2 | ADG019.8-00.7 | 4. | 1414 |
| | | | | | | | | 4. | 2695 |
| 50 | -00 35.6 | 21 48.1 | 27.89 1.19 | 51.91 | E | -0.66 | SG021.8-00.6 | 75. | 408 |
| | | | | | | | BG1830-10 | 34.2 | 408 |
| | | | | | | | AJG079 | 110. | 408 |
| | | | | | | | ADG021.8-00.6 | 46. | 1414 |
| | | | | | | | | 30. | 2695 |
| | | | | | | | | 20. | 5000 |
| | | | | | | | GD021.8-00.6 | 38. | 2700 |
| 51 | -00 30.0 | 16 25.8 | 2.48 .30 | 2.48 | P | -0.2 | ADG016.4-00.5 | 2. | 1414 |
| | | | | | | | | 2. | 2695 |
| | | | | | | | GD016.4-00.5 | 8.1 | 2700 |
| 52 | -00 22.8 | 18 57.4 | 14.24 1.6 | 63.0 | E | | W 39 | | |
| | | | | | | | ADG018.9-00.4 | 18. | 1414 |
| | | | | | | | | 18. | 2695 |
| | | | | | | | | 14. | 5000 |
| | | | | | | | GD018.9-00.4 | 32. | 2700 |
| 53 | -00 19.7 | 18 58.6 | 13.91 1.2 | 46.9 | E | | W 39 | | |
| | | | | | | | BG1824-12. | 8.2 | 408 |
| | | | | | | | ADG019.1-00.3 | 29. | 1414 |
| 54 | -00 22.2 | 16 37.8 | 4.02 1.49 | 4.0 | P | | ADG016.6-00.3 | 4. | 1414 |
| | | | | | | | | 2. | 2695 |
| | | | | | | | | 4. | 5000 |
| | | | | | | | GD016.6-00.3 | 8.4 | 2700 |
| 55 | -00 20.0 | 21 07.8 | .68 .68 | .08 | E | | | | |
| 56 | -00 20.0 | 22 43.8 | 11.7 1.4 | | E | | SG022.-00.5 | 236. | 408 |
| | | | | | | | AJG080 | 100. | 408 |
| | | | | | | | ADG022.8-00.3 | 66. | 1414 |
| | | | | | | | | 51. | 2695 |
| | | | | | | | | 41. | 5000 |
| | | | | | | | GD027.8-00.8 | 69. | 2700 |
| | | | | | | | GS022.8-00.5 | 46. | 5000 |
| 57 | -00 17.4 | 18 10.0 | 15.8 1.1 | 31.4 | E | -0.1 | ADG018.2-00.3 | 27. | 1414 |
| | | | | | | | | 26. | 2695 |
| | | | | | | | | 21. | 5000 |
| | | | | | | | GD023.1-00.3 | 65. | 2700 |
| 58 | -00 16.2 | 23 04.2 | 14.3 1.7 | | E | | AJG089 | 45. | 408 |
| | | | | | | | SG023.1-00.2 | 45. | 408 |
| | | | | | | | ADG023..-00.3 | 50. | 1414 |
| | | | | | | | | 36. | 2695 |
| | | | | | | | | 24. | 5000 |
| | | | | | | | GD023.1-00.3 | 65. | 2700 |
| 59 | -00 12.6 | 19 56.5 | 7.78 1.03 | 7.78 | P | -0.2 | ADG020.0-00.2 | 14. | 1414 |
| | | | | | | | | 11. | 2695 |
| | | | | | | | | 6. | 5000 |
| | | | | | | | GD020.0-00.1 | 14. | 2700 |
| 60 | -00 12.0 | 23 24.0 | 1.70 2.1 | | E | | W41 | | |
| | | | | | | | SG023.3-00.3 | 45. | 408 |
| | | | | | | | ADG023.4-00.2 | 19. | 1414 |
| | | | | | | | | 19. | 2605 |
| | | | | | | | | 15. | 5000 |
| | | | | | | | GD023.4-00.2 | 25. | 2700 |
| | | | | | | | GS023.3-00.3 | 46. | 5000 |
| 61 | -00 12.0 | 24 31.8 | 7.66 0.93 | | E | | SG024.5-00.2 | 3.7 | 408 |
| | | | | | | | GD024.5-00.2 | 19. | 2700 |
| 62 | -00 11.9 | 19 35.7 | 8.71 .82 | 12.25 | P/E | | ADG019.7-00.2 | 16. | 1414 |
| | | | | | | | | 13. | 2695 |
| | | | | | | | | ↓ | 5000 |
| | | | | | | | DG019.6-00.2 | 13. | 2700 |
| 63 | -00 11.37 | 25 22.33 | 23.97 1.84 | 23.97 | P | +0.14 | CUL183-06 | 15. | 80 |
| | | | | | | | | 7.8 | 160 |
| | | | | | | | 3C285 | 17.0 | 159 |
| | | | | | | | CC025-00.1 | 3.8 | 408 |
| | | | | | | | NRA0572 | 25.7 | 750 |
| | | | | | | | | 29.7 | 1400 |
| | | | | | | | ADG025.4-00.2 | 24. | 1414 |
| | | | | | | | | 26. | 2695 |
| | | | | | | | | 23. | 5000 |
| | | | | | | | GS025.3-00.2 | 31. | 5000 |
| | | | | | | | GD025.4-00.2 | 26. | 2700 |
| | | | | | | | SG025.4-00.2 | 12.3 | 408 |
| 64 | -00 11.4 | 26 26.9 | 4.40 .42 | 17.14 | E | -0.2 | ADG026.6-00.1 | 11. | 1414 |
| | | | | | | | | 7. | 2695 |
| | | | | | | | | 10. | 5000 |
| | | | | | | | BKD26.6-00.1 | 3.5 | 1410 |
| | | | | | | | | 5. | 2650 |
| 65 | -00 11.3 | 16 23.6 | 2.78 .33 | 8.56 | E | 0. | ADG016.4-00.2 | 12. | 1414 |
| | | | | | | | | 6. | 2695 |
| | | | | | | | | 9. | 5000 |
| | | | | | | | GD016.3-00.2 | 14. | 2700 |
| 66 | -00 10.2 | 17 10.2 | 1.53 .19 | | E | | ADG017.1-00.1 | 3. | 1414 |
| | | | | | | | | 3. | 2695 |
| | | | | | | | GD017.2-00.20 | 5.8 | 2700 |
| 67 | -00 07.8 | 24 16.2 | 3.48 .42 | | E | | | | |
| 68 | -00 07.8 | 24 40.2 | 9.85 1.2 | | E | | BG1834-07 | 9. | 408 |
| | | | | | | | SG024.7-00.2 | 10.6 | 408 |
| | | | | | | | ADG024+7-00.1 | 23. | 1414 |
| | | | | | | | | 23. | 2695 |
| | | | | | | | | 19. | 5000 |
| | | | | | | | GD024.7-00.1 | 28. | 2700 |
| 69 | -00 06.50 | 20 43.96 | 13.98 1.11 | 19.96 | P/E | -0.08 | BG1826-11 | 18.7 | 408 |
| | | | | | | | ADG020.7-00.1 | 17. | 1414 |
| | | | | | | | | 17. | 2695 |
| | | | | | | | | 16. | 5000 |
| | | | | | | | GD020.7-00.1 | 19. | 2700 |
| 70 | -00 02.17 | 26 06.39 | 6.21 .93 | 8.43 | P/E | -0.5 | ADG026.1-00.0 | 6. | 1414 |
| | | | | | | | | 5. | 2695 |
| | | | | | | | | 4. | 5000 |
| | | | | | | | GD020.4-03.0 | 8.9 | 2700 |
| 71 | -00 00.0 | 22 16.2 | 1.42 .17 | | E | | ADG022.3-00.1 | 1. | 1414 |
| | | | | | | | | 1. | 2695 |
| 72 | -00 00.0 | 23 31.8 | 7.51 0.91 | | E | | SG023.6-00.0 | 11.3 | 408 |
| | | | | | | | ADG023.5-00.0 | 15. | 1414 |
| | | | | | | | | 8. | 2695 |
| | | | | | | | | 13. | 5000 |
| | | | | | | | GD023.5-00.0 | 20. | 2700 |
| | | | | | | | GS023.6-00.0 | 14. | 5000 |
| 73 | +00 01.2 | 21 52.8 | 3.95 .34 | 13.82 | E | -0.6 | ADG021.9-00.0 | 10. | 1414 |
| | | | | | | | | 8. | 2695 |
| | | | | | | | GD021.9+00.0 | 18. | 2700 |
| 74 | 00 04.1 | 24 24.0 | 4.40 .54 | | E | | SG024.4+00.1 | 2.2 | 408 |
| 75 | 00 05.3 | 16 42.5 | 2.29 .75 | 2.29 | P | -0.4 | ADG016.7+00.1 | 3. | 1414 |
| | | | | | | | | 2. | 2695 |
| 76 | 00 05.5 | 24 48.0 | 10.31 1.38 | 12.37 | E | 0. | SG 024.8+00.1 | 12.2 | 408 |
| | | | | | | | ADG024.8+00.1 | 13. | 1414 |
| | | | | | | | | 13. | 2695 |
| | | | | | | | | 13. | 5000 |
| | | | | | | | GD024.8+00.1 | 19. | 2700 |
| 77 | 00°06!0 | 17°37.8 | 1.02±0.12 | | E | | | | |
| 78 | 00 07.8 | 23 55.8 | 2.53 .31 | | E | | ADG020.4+00.1 | 3. | 1414 |
| | | | | | | | | 3. | 2695 |
| 79 | 00 07.8 | 23 40.2 | 4.81 .58 | | E | | SG023.7+00.2 | 236. | 408 |
| | | | | | | | GD023.6+00.1 | 23. | 2700 |
| | | | | | | | GS023.7+00.2 | 14. | 5000 |
| 80 | 00 07.8 | 23 55.8 | 2.53 0.31 | | E | | ADG023.9+00.2 | 2. | 1414 |
| | | | | | | | | 3. | 2695 |
| | | | | | | | | 1.9 | 5000 |
| | | | | | | | GD023.9+00.1 | 3.2 | 2700 |
| 81 | 00 08.1 | 19 23.1 | 4.05 .66 | 12.1 | E | -0.8 | ADG019.5+00.1 | 3. | 1414 |
| | | | | | | | | 3. | 2695 |
| | | | | | | | GD019.5+00.1 | 5.6 | 2700 |
| 82 | 00 10.8 | 25 46.9 | 10.29 .91 | 20.5 | E | -0.3 | ADG025.8+00.2 | 14. | 1414 |
| | | | | | | | | 14. | 2695 |
| | | | | | | | | 13. | 5000 |
| | | | | | | | GD025.8+00.2 | 14. | 2700 |
| 83 | 00 10.2 | 16 10.2 | 1.28 .16 | 1.28 | P | | | | |
| 84 | 00 12.4 | 24 28.8 | 7.47 1.26 | 10.2 | P/E | 0. | SG024.5+00.2 | 14.1 | 408 |
| | | | | | | | ADG024.5+00.2 | 18. | 1414 |
| | | | | | | | | 18. | 2695 |
| | | | | | | | | 12. | 5000 |
| | | | | | | | GD024.5+00.2 | 18. | 2700 |
| 85 | 00 17.2 | 25 15.6 | 2.73 .51 | 4.17 | E | -0.7 | SG025.3+00.3 | 6.4 | 408 |
| | | | | | | | ADG025.3+00.3 | 3. | 1414 |
| | | | | | | | | 2. | 2695 |
| | | | | | | | GD025.3+00.3 | 4.2 | 2700 |
| 86 | 00 20.53 | 18 44.72 | 14.04 1.0 | 29.5 | E | -0.5 | AJG078 | 38.1 | 408 |
| | | | | | | | BG1821.-12. | 28.2 | 408 |
| | | | | | | | ADG018.8+00.3 | 33. | 1414 |
| | | | | | | | | 19. | 2695 |
| | | | | | | | | 12. | 5000 |
| | | | | | | | GD018.8+00.3 | 12. | 2700 |
| 87 | 00 24.0 | 26 31.8 | 1.54 .19 | 1.54 | P | +0.6 | ADG026.6+00.4 | 2. | 1414 |
| | | | | | | | | 2. | 2695 |
| | | | | | | | GD026.5+00.4 | 3.2 | 2700 |
| 88 | 00 28.2 | 23 48.0 | .66 .08 | | E | | | | |
| 89 | 00 28.2 | 24 52.2 | 1.29 .16 | | E | | | | |
| 90 | 00 33.0 | 23 06.1 | 2.55 .36 | 2.55 | P | -0.3 | BG1828-08 | 2.4 | 408 |
| | | | | | | | SG023.1+00.6 | 6. | 408 |
| | | | | | | | ADG023.1+00.5 | 2. | 1414 |
| | | | | | | | | 2. | 2695 |
| | | | | | | | GD023.1+00.6 | 2.8 | 2700 |
| 91 | 00 35.1 | 24 35.5 | 7.43 .61 | 23.4 | E | -0.33 | AJG083 | 20. | 408 |
| | | | | | | | SG024.7+00.6 | 27. | 408 |
| | | | | | | | ADG024.6+00.5 | 14. | 1414 |
| | | | | | | | | 11. | 2695 |
| | | | | | | | | 13. | 5000 |
| 92 | 00°48!0 | 25°43!8 | .63± .08 | | P | | | | |
| 93 | 00 50.30 | 16 56.86 | 39.02 2.9 | 151.3 | E | -0.5 | S49,NGC6611, | W37 | |
| | | | | | | | BG1816-14 | 33.7 | 408 |
| | | | | | | | SG016.9+00.7 | 193. | 408 |
| | | | | | | | ADG017.0+00.8 | 134. | 1414 |
| | | | | | | | | 107. | 2695 |
| | | | | | | | | 103. | 5000 |
| | | | | | | | GD017.0+00.9 | 169. | 2700 |
| | | | | | | | GS016.9+00.8 | 114. | 5000 |
| | | | | | | | MH016.9+00.8 | 52.6 | 5000 |
| | | | | | | | GM42 | 45.0 | 5000 |
| 94 | 01 10.6 | 18 19.1 | 1.12 .14 | 1.95 | E | +0.6 | CC018+01.0 | 1.04 | 408 |
| | | | | | | | ADG018.7+01.2 | 4. | 1414 |
| | | | | | | | | 3. | 2695 |
| 95 | 01 14.5 | 20 09.8 | .52 .06 | 1.87 | E | | | | |
| 96 | 01 25.8 | 17 42.0 | .94 .11 | | E | | | | |
| 97 | 01 26.1 | 26 23.3 | 1.05 .10 | 1.05 | P | | | | |
| 98 | 01 27.2 | 20 51.1 | .28 .06 | .62 | E | | | | |
| 99 | 01 37.8 | 17 01.4 | 2.40 .22 | 15.1 | E | | ADG017.0+01.6 | 4. | 1414 |
| | | | | | | | | 4. | 2695 |
| | | | | | | | GD017.0+01.7 | 3.7 | 2700 |
| 100 | 01 43.6 | 25 16.2 | .51 .06 | | E | | | | |
| 101 | 01 44.3 | 22 20.0 | .58 .06 | .58 | P | -0.1 | CC022+01.7 | 0.68 | 408 |
| 102 | 01 46.2 | 18 46.2 | 8.17 .99 | | E | | ADG018.7+01.8 | 14. | 1414 |
| | | | | | | | | 14. | 2695 |
| | | | | | | | GD018.8+01.8 | 69. | 2700 |
| | | | | | | | GS018.8+01.8 | 70. | 5000 |
| 103 | 01 54.0 | 18 10.2 | 6.87 .84 | | E | | SG018.2+01.9 | 223. | 408 |
| | | | | | | | ADG018.2+01.9 | 8. | 1414 |
| | | | | | | | | 6. | 2695 |
| | | | | | | | | 6. | 5000 |
| | | | | | | | GD018.2+01.9 | 57. | 2700 |
| | | | | | | | GS018.2+01.9 | 70. | 5000 |
| 104 | 01 57.03 | 21 02.61 | 7.09 .51 | 7.09 | P | -0.56 | CUL1819-09. | 11. | 80 |
| | | | | | | (v>400) | | 11.1 | 160 |
| | | | | | | | CC021+02.0 | 10.66 | 408 |
| | | | | | | 0. | BG1819-09 | 8.6 | 408 |
| | | | | | | (<400) | ADG021.0+02.0 | 6. | 1414 |
| | | | | | | | | 4. | 2695 |
| | | | | | | | OU-033 | 4.7 | 1414 |
| | | | | | | | | 3.9 | 2650 |
| | | | | | | | | 2.0 | 612 |
| 105 | 01 58.2 | 17 30.0 | .47 .06 | | E | | | | |
| 106 | 01 58.2 | 18 37.8 | 12.12 .15 | | VE | | S51,NGC6604, | W35 | |
| | | | | | | | BG1815-11A | 6.0 | 408 |
| | | | | | | | SG018.5+01.9 | 223. | 408 |
| | | | | | | | ADG018.6+1.9 | 122. | 1414 |
| | | | | | | | | 97. | 2695 |
| | | | | | | | | 94. | 5000 |
| | | | | | | | GD018.5+02.0 | 93. | 2700 |
| | | | | | | | GS018.5+02.0 | 70. | 5000 |
| 107 | 02°09!8 | 19°13!2 | 2.71±.52 | 2.71 | P | -0.8 | BG1815-11B | 4.7 | 408 |
| | | | | | | | | ADG019.2+02.1 | 2. | 1414 |
| | | | | | | | | | 2. | 2695 |
| | | | | | | | GD019.2+2.2 | | 6.3 | 2700 |
| | | | | | | | GS019.2+07.2 | | 0.56 | 5000 |
| 108 | 02 12.0 | 22 31.8 | .51 .06 | | E | | | | | |
| 109 | 02 12.0 | 23 12.0 | .44 .05 | .44 | P | | | | | |
| 110 | 02 13.8 | 17 18.0 | .72 .09 | | E | | | | | |
| 111 | 02 14.9 | 22 02.4 | .30 .09 | .30 | P | | | | | |
| 112 | 02 16.5 | 23 42.1 | .33 .03 | 1.5 | VE | | | | | |
| 113 | 02 17.6 | 20 42.0 | 1.03 .60 | 1.03 | P | -0.56 | CUL1817-09 | <7. | 80 |
| | | | | | | | | | 3.1 | 160 |
| | | | | | | | BG1817-09 | | 1.9 | 408 |
| | | | | | | | CC020+02.3 | | 2.1 | 408 |
| 114 | 02 31.7 | 25 25.2 | .74 .07 | .74 | P | | OU-043 | | 0.7 | 1415 |
| 115 | 02 32.5 | 23 12.8 | .41 .06 | .41 | P | | | | | |
| 116 | 02 34.2 | 16 22.2 | .33 .04 | | E | | | | | |
| 117 | 02 35.0 | 24 48.5 | .27 .03 | 1.22 | VE | | | | | |
| 118 | 02 41.5 | 26 12.5 | .48 .05 | 1.08 | E | | | | | |
| 119 | 02 52.4 | 20 17.9 | .52 .06 | .52 | P | | | | | |
| 120 | 02 57.9 | 21 05.6 | .63 .06 | 2.37 | E | | | | | |
| 121 | 03 20.0 | 21 07.8 | .27 .03 | .27 | P | | | | | |
| 122 | 03 22.93 | 26 33.82 | .96 .08 | .96 | P | | OU-041 | | 1.0 | 1415 |
| 123 | 03 28.2 | 25 04.2 | .28 .03 | | E | | | | | |
| 124 | 03 28.97 | 21 47.95 | .59 .07 | .59 | P | | | | | |
| 125 | 03 40.2 | 22 24.0 | .42 .05 | | E | | | | | |
| 126 | 03 43.8 | 26 24.0 | .26 .03 | | E | | OU-039.1 | | 0.4 | 1415 |
| 127 | 03 48.2 | 23 09.5 | .37 .07 | .37 | P | | | | | |
| 128 | 03 52.2 | 23 55.8 | .28 .03 | | E | | | | | |
| 129 | 03 53.5 | 25 42.1 | .47 .05 | .47 | P | | | | | |
| 130 | 03 57.3 | 20 47.9 | .29 .05 | .29 | P | | | | | |
| 131 | 04 24.5 | 24 57.7 | .76 .06 | .76 | P | | | | | |
| 132 | 04 31.8 | 26 52.2 | .35 .04 | | E | | | | | |
| 133 | 04 36.9 | 20 21.3 | .36 .04 | .36 | P | | | | | |
| 134 | 04 38.5 | 26 10.0 | .20 .03 | .41 | E | | | | | |
| 135 | 04 52.8 | 21 29.4 | .21 .02 | .72 | E | | | | | |
| 136 | 04 53.00 | 25 24.55 | 1.06 .08 | 1.06 | P | -0.8 | CUL1817-04 | 6. | 80 |
| | | | | | | | | | 7.0 | 160 |
| | | | | | | | 4C-04.67 | | 4.6 | 179 |
| | | | | | | | BG1817-04 | | 2.1 | 408 |
| | | | | | | | OU-029 | | 0.7 | 1415 |
| 137 | 05 03.0 | 26 43.6 | .14 .02 | .28 | E | | | | | |
| 138 | 05 05.7 | 21 53.3 | .17 .02 | .87 | E | | | | | |
| 139 | 05 07.8 | 23 16.2 | .26 .03 | .26 | P | | | | | |
| 140 | 05°12!0 | 20°20!0 | .29± .04 | | E | | OU-011.2 | | 1.0 | 1415 |
| 141 | 05 19.3 | 23 50.8 | .43 .10 | .43 | P | -0.8 | 4C-05.75 | | 2.2 | 179 |
| 142 | 05 20.0 | 25 55.8 | .33 .04 | | E | | | | | |
| 143 | 05 23.80 | 22 26.10 | 1.60 .12 | 1.6 | P | -0.4 | 4C-06.53 | | 3.3 | 179 |
| | | | | | | | OU-016 | | 1.27 | 1415 |
| 144 | 05 31.18 | 26 08.75 | .87 .10 | .87 | P | -0.7 | CUL1816-03 | 8. | 80 |
| | | | | | | | | | 5.0 | 160 |
| | | | | | | | 4C-03.67 | | 4.5 | 179 |
| | | | | | | | BG1816-03 | | 2.9 | 408 |
| 145 | 05 40.2 | 25 07.8 | .27 .03 | .27 | P | | | | | |
| 146 | 05 42.1 | 25 36.3 | .21 .05 | .26 | P/E | | | | | |
| 147 | 05 46.33 | 26 35.41 | 2.17 .16 | 2.17 | P | | OU-027 | | 2.3 | 1415 |
| 148 | 05 46.72 | 26 35.75 | 1.54 .13 | 1.54 | P | | | | | |
| 149 | 06 00.7 | 28 46.1 | .14 .02 | .29 | E | | OU-033.1 | | 0.3 | 1415 |
| 150 | 06 09.9 | 29 55.6 | .36 .03 | .53 | E | | | | | |
| 151 | 06 29.0 | 25 15.6 | .31 .04 | .31 | P | | | | | |
| 152 | 06 36.1 | 28 43.3 | .17 .02 | .39 | E | | OU-030 | | 0.3 | 1415 |
| 153 | 06 44.6 | 29 26.9 | .14 .02 | .24 | E | | | | | |
| 154 | 06 50.0 | 26 22.8 | .32 .04 | .32 | P | | OU-020.6 | | 0.6 | 1415 |
| 155 | 06 57.9 | 23 08.8 | .40 .03 | .40 | P | | | | | |
| 156 | 07 04.0 | 28 08.4 | .32 .03 | .39 | E | | | | | |
| 157 | 07 15.0 | 24 49.6 | .40 .05 | .40 | P | -0.8 | 4C-03.66 | | 2.3 | 179 |
| 158 | 07 17.9 | 23 52.7 | .26 .03 | 1.57 | VE | | OU-009 | | 0.3 | 1415 |
| 159 | 07 20.1 | 23 12.9 | .29 .04 | .29 | P | | | | | |
| 160 | 07 21.8 | 26 47.6 | .30 .03 | .91 | VE | | OU-018 | | 0.5 | 1415 |
| 161 | 07 41.4 | 27 56.6 | .28 .03 | .28 | P | | | | | |
| 162 | 07 43.5 | 24 45.4 | .21 .02 | .48 | E | | | | | |
| 163 | 07 48.0 | 28 37.8 | .28 .03 | | E | | | | | |
| 164 | 07 52.3 | 27 44.3 | .22 .05 | .22 | P | | | | | |
| 165 | 08 01.5 | 23 29.3 | .75 .05 | .86 | P/E | | OU-004.7 | | 0.9 | 1415 |
| 166 | 08 05.5 | 25 37.3 | .27 .03 | 1.45 | VE | | OU-011.1 | | 1.3 | 1415 |
| 167 | 08 07.52 | 28 47.19 | .84 .07 | 1.10 | P/E | -0.8 | 4C+00.68 | | 4.8 | 179 |
| | | | | | | | | | 50. | 38 |
| | | | | | | | OU+021 | | 1.4 | 1415 |
| | | | | | | | CUL1812+00 | | 10. | 80 |
| | | | | | | | | | 7.2 | 160 |
| 168 | 08 07.8 | 28 48.0 | 1.09 .13 | 1.09 | P | | | | | |
| 169 | 08 15.9 | 33 50.5 | .25 .03 | .54 | E | | OU+035.5 | | 0.37 | 1415 |
| 170 | 08 20.0 | 32 23.7 | .28 .06 | .28 | P | | OU+030 | | 0.37 | 1415 |
| 171 | 08 27.7 | 31 15.0 | .25 .04 | .29 | P/E | | | | | |
| 172 | 08 39.7 | 31 39.4 | .26 .03 | .37 | E | | | | | |
| 173 | 08 46.1 | 33 07.7 | .23 .03 | .55 | VE | | | | | |
| 174 | 08 51.9 | 29 47.8 | .21 .03 | .39 | E | | | | | |
| 175 | 09 04.9 | 34 49.5 | .28 .03 | .28 | P | | | | | |
| 176 | 09 18.2 | 32 14.7 | .56 .05 | .56 | P | -1.0 | CUL1814+03 | 12. | 80 |
| | | | | | | | | | 5.9 | 160 |
| | | | | | | | 4C+03.40 | | 4.5 | 179 |
| | | | | | | | OU+025 | | 0.43 | 1415 |

1979A&AS...38..251S



Table 1 *(continued)*

| No. | b | l | $S_p$(Jy beam) | S(Jy) | Type | α | Identification Name | Flux (Jy) | Freq. (MHz) |
|---|---|---|---|---|---|---|---|---|---|
| 177 | 09°19!9 | 26°53!4 | .36± .04 | 1.31 | VE | | | | |
| 178 | 09 26.7 | 30 45.6 | .27 .04 | .45 | E | | OU+019.3 | 0.13 | 1415 |
| 179 | 09 30.5 | 28 56.6 | .25 .04 | .38 | E | | | | |
| 180 | 09 51.9 | 27 30.0 | .66 .08 | | E | | | | |
| 181 | 10 09.8 | 32 21.0 | .25 .05 | .37 | E | | | | |
| 182 | 10 15.8 | 31 40.7 | .30 .04 | .30 | P | | | | |
| 183 | 10 36.45 | 32 45.02 | 2.29 .19 | 2.29 | P | -1.0 | CUL1810+04 | 11. | 80 |
| | | | | | | | | 10.3 | 160 |
| | | | | | | | 4C+04.63 | 9.4 | 179 |
| | | | | | | | OU+019 | 2.0 | 1415 |
| 184 | 10 43.0 | 30 14.1 | .45 .05 | .68 | E | | | | |
| 185 | 10 52.2 | 28 12.0 | .55 .07 | .55 | P | | | | |
| 186 | 10 55.2 | 31 54.6 | .29 .03 | .58 | E | | | | |
| 187 | 10 56.4 | 33 00.0 | .35 .04 | | E | | | | |
| 188 | 10 56.6 | 28 23.9 | .98 .10 | 1.46 | E | -1.0 | PKS1801+01 | 5.5 | 408 |
| | | | | | | | | 1.4 | 1410 |
| | | | | | | | | 0.9 | 2650 |
| 189 | 10 58.7 | 34 18.6 | .40 .05 | .40 | P | | | | |
| 190 | 11 10.0 | 26 47.5 | .42 .06 | 2.54 | VE | | | | |
| 191 | 11 29.9 | 27 16.2 | .24 .03 | .70 | VE | | | | |
| 192 | 11 39.5 | 26 00.7 | .27 .04 | .27 | P | | | | |
| 193 | 11 46.0 | 28 49.1 | .58 .05 | .58 | P | -0.6 | 4C+01.54 | 2.0 | 179 |
| 194 | 11 48.9 | 34 37.3 | .39 .04 | .47 | P/E | +0.5 | PKO34+11.1 | 1.30 | 10630 |
| | | | | | | | | 1.06 | 3240 |
| | | | | | | | | 1.23 | 6630 |
| | | | | | | | (Planetary nebula) | | |
| 195 | 12 49.08 | 31 20.89 | .70 .06 | .70 | P | -1.0 | 4C+04.62 | 2.9 | 179 |
| 196 | 12 09.4 | 32 51.6 | .40 .05 | .40 | P | | | | |
| 197 | 12 19.2 | 27 13.6 | .17 .02 | | E | | | | |
| 198 | 12 14.1 | 30 47.7 | .24 .04 | .24 | P | -1. | 4C+03.39 | 2.1 | 179 |
| 199 | 12 22.0 | 33 11.2 | .59 .07 | .59 | P | | | | |
| 200 | 12 30.7 | 32 39.0 | .37 .04 | .37 | P | | | | |
| 201 | 12 30.9 | 32 38.4 | .59 .06 | .59 | P | | | | |
| 202 | 12 37.05 | 33 44.16 | 1.29 .10 | 1.29 | P | -0.8 | 4C+06.64 | 7.0 | 179 |
| | | | | | | | 4CP06.64 | 6.0 | 178 |
| | | | | | | | OU+009 | 1.21 | 1415 |
| | | | | | | | CUL1805+06 | 10. | 80 |
| | | | | | | | | 6.2 | 160 |
| 203 | 12 47.7 | 30 14.5 | .29 .03 | 1.04 | VE | | | | |
| 204 | 12 48.1 | 34 16.3 | .17 .02 | .37 | E | | | | |
| 205 | 13 07.7 | 28 05.7 | .28 .06 | .28 | P | | | | |
| 206 | 13 20.0 | 31 16.2 | .29 .04 | .29 | P | | | | |
| 207 | 13 24.6 | 27 48.1 | .41 .05 | .41 | P | -0.9 | 4C+01.53 | 2.8 | 179 |
| 208 | 13 25.2 | 32 19.7 | .25 .04 | .25 | P | | | | |
| 209 | 13°31!8 | 29°43!8 | .33± .04 | .33 | P | -3. | PKS1755+03. | 15. | 408 |
| | | | | | | | | 0.5 | 1410 |
| 210 | 13 32.3 | 31 47.8 | .17 .02 | .72 | P | | | | |
| 211 | 13 45.62 | 29 54.11 | .72 .06 | .72 | P | | | | |
| 212 | 14 15.37 | 28 09.00 | 1.13 .08 | 1.13 | P | -1.0 | 4C+02.45 | 4.6 | 179 |
| | | | | | | | PKS1749+023 | 0.55 | 2700 |
| 213 | 14 19.0 | 28 38.0 | .43 .04 | 1.02 | E | | | | |
| 214 | 14 22.85 | 32 39.31 | .83 .06 | .83 | P | -0.8 | CUL1757+06 | 11. | 80 |
| | | | | | | | | 2.8 | 160 |
| | | | | | | | 4CP06.63 | 4.0 | 178 |
| | | | | | | | 4C+06.63 | 4.4 | 179 |
| | | | | | | | OT+096.1 | 1.15 | 1415 |
| 215 | 14 35.8 | 30 58.6 | .49 .05 | .49 | P | | | | |
| 216 | 14 55.8 | 30 19.8 | .57 .06 | | E | | PKS1751+04 | 7.0 | 408 |
| | | | | | | | | 1.5 | 1410 |
| | | | | | | | | 0.3 | 2650 |
| 217 | 14 57.42 | 28 46.42 | 1.63 .12 | 1.63 | P | -0.7 | 4C+03.38 | 6.3 | 179 |
| | | | | | | | OT+080 | 0.67 | 1415 |
| | | | | | | | PKS1748+031 | 0.80 | 2700 |
| | | | | | | | CUL1748+03 | 9. | 80 |
| | | | | | | | | 8.1 | 160 |
| 218 | 14 58.83 | 30 52.44 | .85 .06 | .85 | P | -047 | PKS1751+050 | 0.7 | 2700 |
| | | | | | | | | 0.45 | 5000 |
| 219 | 15 13.8 | 26 23.6 | .19 .03 | .43 | | | | | |
| 220 | 15 23.38 | 33 35.41 | 1.71 .12 | 1.71 | P | -0.7 | CUL1755+07 | <9. | 80 |
| | | | | | | | | 5.0 | 160 |
| | | | | | | | 4C+07.47 | 5.1 | 179 |
| | | | | | | | 4CP07.47 | 4.5 | 178 |
| | | | | | | | NRAO541 | 1.24 | 750 |
| | | | | | | | OT+091 | 0.75 | 1415 |
| 221 | 15 28.0 | 29 03.1 | .39 .04 | .39 | P | | OT+076.1 | 0.29 | 1415 |
| 222 | 15 33.7 | 36 33.6 | .53 .06 | .78 | E | -0.7 | 4C+08.51 | 3.5 | 179 |
| | | | | | | | 4CP08.51 | 3.9 | 178 |
| | | | | | | | OT+093 | 0.40 | 1415 |
| 223 | 15 52.6 | 29 18.2 | .37 .05 | .37 | P | | | | |
| 224 | 15 58.8 | 31 44.2 | .71 .09 | | E | | OT+083.2 | 1.09 | 1415 |
| | | | | | | | PKS1749+062 | 0.81 | 2700 |
| | | | | | | | | 0.54 | 5000 |
| 225 | 16 50.5 | 27 21.6 | .31 .05 | .31 | P | | OT+064 | 0.22 | 1415 |
| 226 | 16 54.5 | 30 25.2 | .34 .05 | .47 | E | -0.7 | 4C+05.68 | 2.3 | 179 |
| 227 | 17 04.6 | 29 00.4 | .31 .04 | .31 | P | | | | |
| 228 | 17 07.3 | 34 44.1 | .53 .06 | 1.06 | E | -0.7 | OT+084 | 0.92 | 1415 |
| | | | | | | | PKS1750+093 | 0.58 | 2700 |
| | | | | | | | | 0.43 | 5000 |
| 229 | 17 12.6 | 27 36.6 | .39 .06 | .39 | P | -0.6 | PKS1738+032 | 0.27 | 2700 |
| 230 | 17 27.3 | 33 43.8 | .25 .04 | .25 | P | | | | |
| 231 | 17 34.6 | 26 40.9 | .54 .05 | .54 | P | -1.1 | PKS1735+026 | 0.26 | 2700 |
| 232 | 17 35.1 | 34 46.1 | .60 .06 | .60 | P | | | | |
| 233 | 17 38.1 | 27 47.5 | .34 .05 | .61 | E | | | | |
| 234 | 17 40.0 | 35 00.0 | .77 .09 | .77 | P | +0.7 | GC1749+09 | 1.83 | 1000 |
| 235 | 17°43!8 | 27°52!2 | .43± .06 | .43 | P | | | | |
| 236 | 17 54.8 | 32 15.2 | .98 .08 | .98 | P | -0.8 | CUL1743+07 | 10. | 80 |
| | | | | | | | | 6.6 | 160 |
| | | | | | | | 4C+07.46 | 4.1 | 179 |
| | | | | | | | 4CP07.46 | 4.2 | 178 |
| 237 | 17 55.07 | 27 28.72 | 1.53 .09 | 1.53 | P | -0.6 | CUL1735+03 | 7. | 80 |
| | | | | | | | | 6.4 | 160 |
| | | | | | | | 4C+03.37 | 3.6 | 179 |
| | | | | | | | OT+059 | 1.29 | 1425 |
| | | | | | | | PKS1735+034 | 0.80 | 2700 |
| 238 | 17 55.6 | 33 32.7 | .40 .10 | .40 | P | | OTO76.3 | 0.54 | 1415 |
| 239 | 18 11.2 | 33 39.7 | .72 .07 | .72 | P | -0.8 | CUL1745+08 | 10. | 80 |
| | | | | | | | | 4.6 | 160 |
| | | | | | | | 4C+08.5 | 3.5 | 179 |
| | | | | | | | 4CP08.5 | 4.2 | 178 |
| | | | | | | | OT+075 | 0.85 | 1415 |
| 240 | 18 13.2 | 30 24.0 | 1.05 .08 | 1.05 | P | -0.8 | CUL1739+06 | 18. | 80 |
| | | | | | | | | 5.9 | 160 |
| | | | | | | | 4C+06.62 | 4.8 | 179 |
| | | | | | | | 4CP06.62 | 4.1 | 178 |
| | | | | | | | OP+066.6 | 1.12 | 1415 |
| 241 | 18 17.6 | 28 54.2 | .27 .02 | .64 | E | | | | |
| 242 | 18 18.1 | 34 21.6 | 1.04 .09 | 1.04 | P | -0.8 | CUL1746+09 | 11. | 80 |
| | | | | | | | | 3.5 | 160 |
| | | | | | | | 4C+09.56 | 6.8 | 179 |
| | | | | | | | 4CP09.56 | 6.1 | 178 |
| | | | | | | | OP+079 | 1.6 | 1415 |
| 243 | 18 25.1 | 32 10.5 | .27 .03 | 1.14 | E | | | | |
| 244 | 18 41.7 | 32 46.1 | .58 .05 | .80 | E | -0.7 | 4C+08.49 | 3.3 | 179 |
| | | | | | | | 4CP08.49 | 4.0 | 178 |
| | | | | | | | OT+069 | 0.35 | 1415 |
| 245 | 18 48.0 | 30 40.2 | .31 .04 | .31 | P | | | | |
| 246 | 18 56.2 | 31 32.9 | .24 .03 | .60 | E | | | | |
| 247 | 19 01.4 | 29 28.2 | .53 .05 | .53 | P | -0.9 | 4C+05.67 | 3.7 | 179 |
| 248 | 19 21.6 | 30 08.1 | .76 .07 | 1.16 | E | -0.5 | OT+058.3 | 0.85 | 1415 |
| | | | | | | | PKS1743+063 | 0.75 | 2700 |
| | | | | | | | | 0.62 | 5000 |
| 249 | 19 28.2 | 31 55.8 | .37 .03 | .37 | P | | | | |
| 250 | 19 52.2 | 32 52.2 | .31 .04 | | E | | | | |

NOTES TO TABLE 1

Column 1: Running number of the source.
Column 2: New galactic latitude.
Column 3: New galactic longitude.
Column 4: Peak flux density in Jy/beam with estimated error.
Column 5: Total flux density. This is given only when gaussian extents (see the text) of the source are known.
Column 6: Designation of point (P) or extended (E) sources. VE designates very extended sources with convolved extents greater than 20′; P/E slightly extended sources with extents $<11'$.
Column 7: Spectral index.
Column 8: Identification with sources in other lists and their flux densities (in Jy) at corresponding frequencies (MHz).

References are:


ADG: Altenhoff, Downes, Goad, Maxwell and Rinehart: 1970, *Astron. Astrophys. Suppl.* **1**, 319, 1970.

AJG: Green, A.J.: 1974, *Astron. Astrophys. Suppl.* **18**, 267, 1974.

BG: Fanti, Felli, Ficarra, Salter, Toffani and Tomasi: *Astron. Astrophys. Suppl.* **16**, 43, 1974.

BK: Beard and Kerr: *Aust. J. Phys.* **22**, 121, 1969.

CC: Clark and Clifford: *Aust. J. Phys.* **27**, 713, 1973.

CUL: Slee: *Aust. J. Phys. Suppl.* **43**, 1, 1977.

GD: Goss and Day: *Aust. J. Phys. Suppl.* **13**, Apr. 1970.

GS: Goss and Shaver: *Aust. J. Phys. Suppl.* **14**, 1, 1970.

NRAO: Pauliny-Toth, Wade and Heeschen: *Ap. J. Suppl.* **116**, 1966.

OT, OU: Fitch, Dixon and Kraus: *Astron. J.* **74**, 612, 1970;
Ehman, Dixon and Kraus: *Astron. J.* **75**, 351, 1970;
Ehman, Dixon, Ramakrishna and Kraus: *Astron. J.* **79**, 144, 1974;
Rinsland, Dixon, Gearhart and Kraus: *Astron. J.* **79**, 1129, 1974.


Table 2 Integrated source counts per square degree

| Limiting flux $S_o$ Jy | N($S_p$) (Present counts,b)6*) All sources* | Point sources | N($S_o$) (Maslowski 1973) |
|---|---|---|---|
| 1.4 | 0.07±0.02 | 0.04±0.02 | 0.03±0.01 |
| 1.0 | .16 .04 | .07 .02 | .07 .01 |
| .7 | .26 .04 | .13 .03 | .11 .01 |
| .5 | .41 .06 | .22 .04 | .19 .02 |
| .4 | .52 .07 | .30 .05 | .27 .02 |
| .35 | .62 .07 | .34 .05 | .34 .03 |
| .3 | .67 .07 | .40 .06 | .42 .03 |
| .25 | .77 .08 | .48 .06 | .53 .04 |

*P and E sources with $S_p > S_o$ in Table 1

Table 3 List of sources in the peculiar association at 033+11.5

| Designation in Fig. 5 | l | b | RA (1950) | Dec (1950) | $S_p$ (Jy beam) | S (Jy) | α | No. in Table 1 |
|---|---|---|---|---|---|---|---|---|
| A | 33°44!16 | 12°37!05 | $18^h05^m20^s.3$ | 06°25'01" | - | 1.29±0.10 | -0.8 | 202 |
| B | 32 38.4 | 12 30.9 | 18 05 27.9 | 06 11 54 | - | .59 .06 | | 201 |
| C | 33 11.2 | 12 22.0 | 18 05 17.2 | 05 48 59 | - | .59 .07 | | 199 |
| D | 32 51.6 | 12 09.4 | 18 05 22.2 | 05 26 30 | - | .40 .05 | | 196 |
| E | 32 35.2 | 12 10.0 | 18 04 56.3 | 05 12 08 | - | .22 .03 | | - |
| F | 32 39.0 | 12 30.7 | 18 03 45.3 | 05 24 27 | - | .37 .04 | | 200 |
| G | 32 45.02 | 10 36.45 | 18 10 47.5 | 04 38 38 | - | 2.29 .19 | -1.0 | 183 |
| H | 33 00.0 | 10 56.4 | 18 10 04.5 | 05 01 40 | .35±.04 | - | | 187 |

Figure 1 a-f: Contour maps of distribution of the main beam brightness temperature $T_b$ in the NPS region in the galactic coordinate system. The whole region is divided into six parts, a-f, which overlap slightly each other. The $T_b$ values are indicated in deg. K on the contours. Some contours are indicated with arrows pointing downhill. Contours at $T_b = 1.2$, 3, 6, 10 and 20 K are hatched downhill. Declination and right ascension (1950) are also indicated.

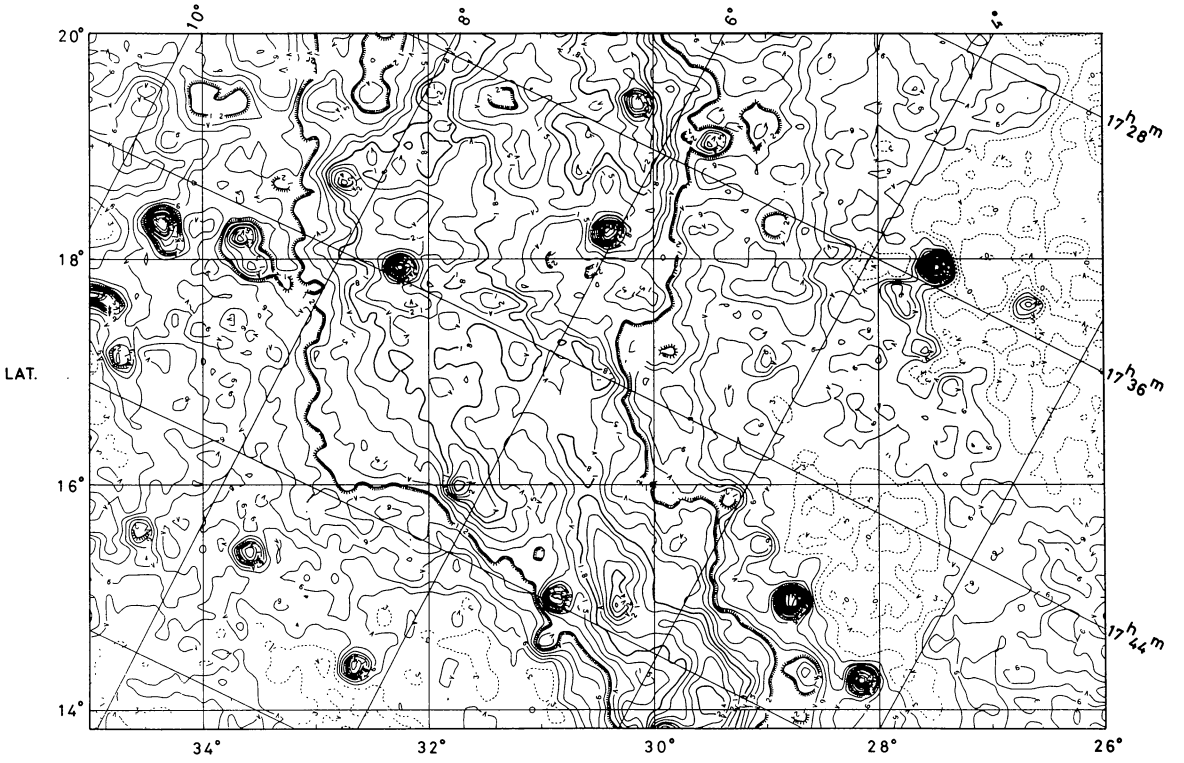


Figure 1a

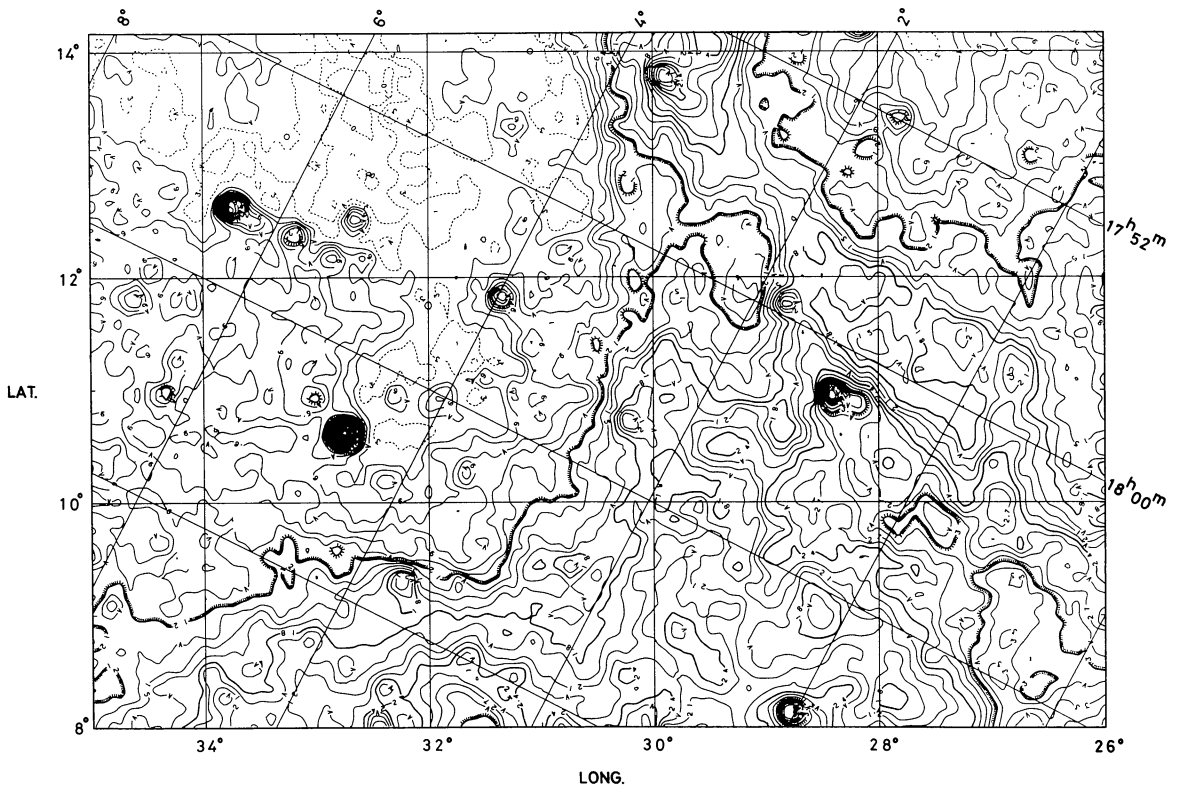


Figure 1b

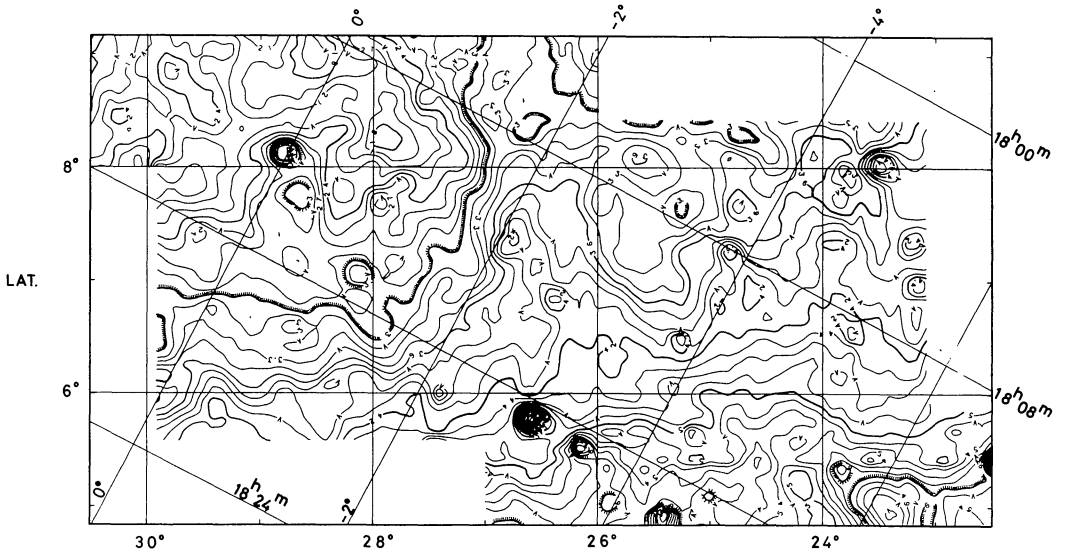


Figure 1c

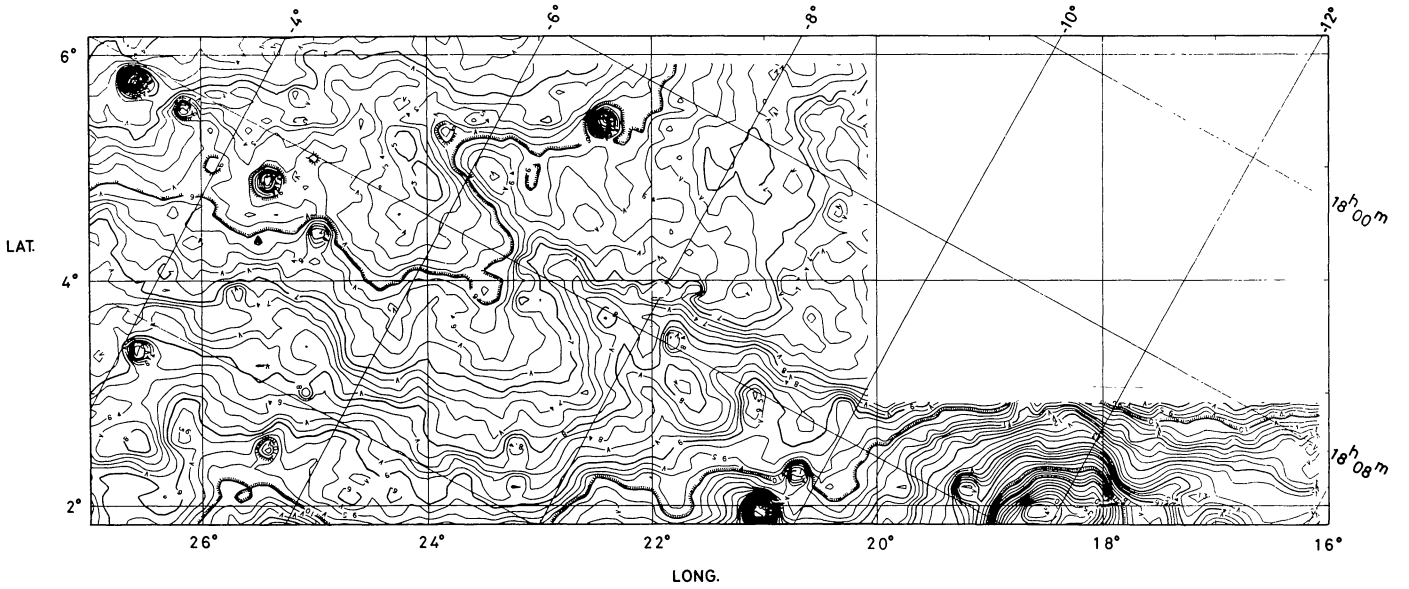


Figure 1d

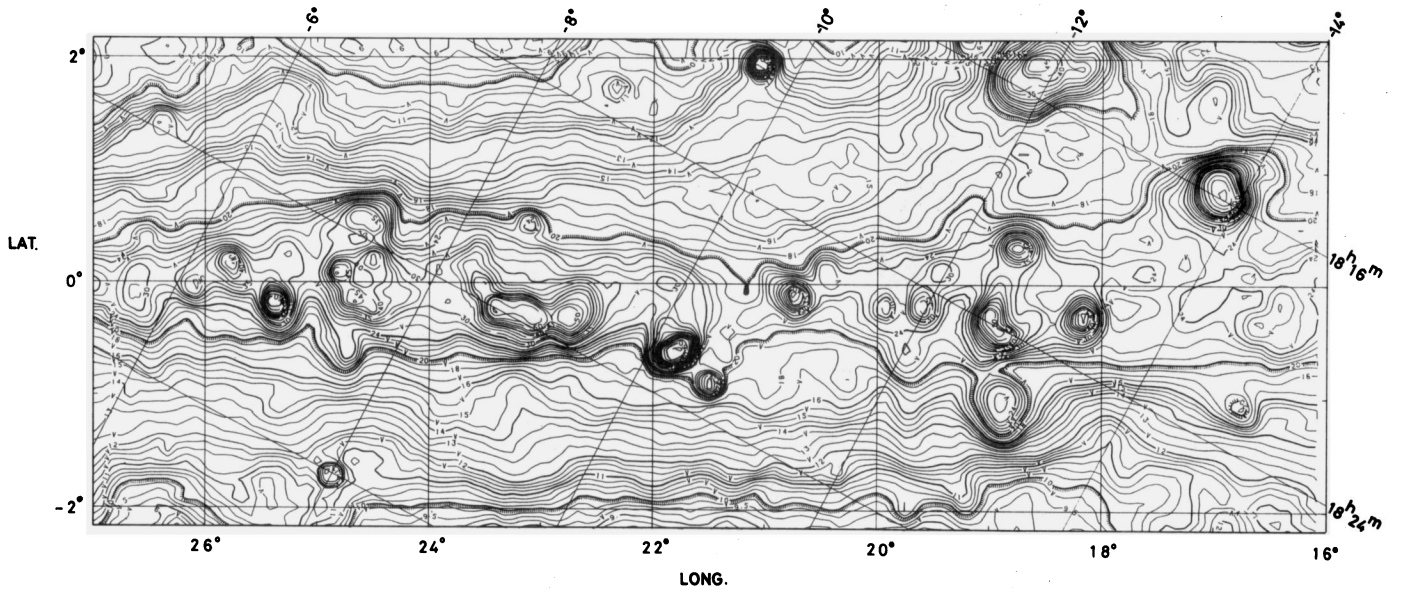


Figure 1e

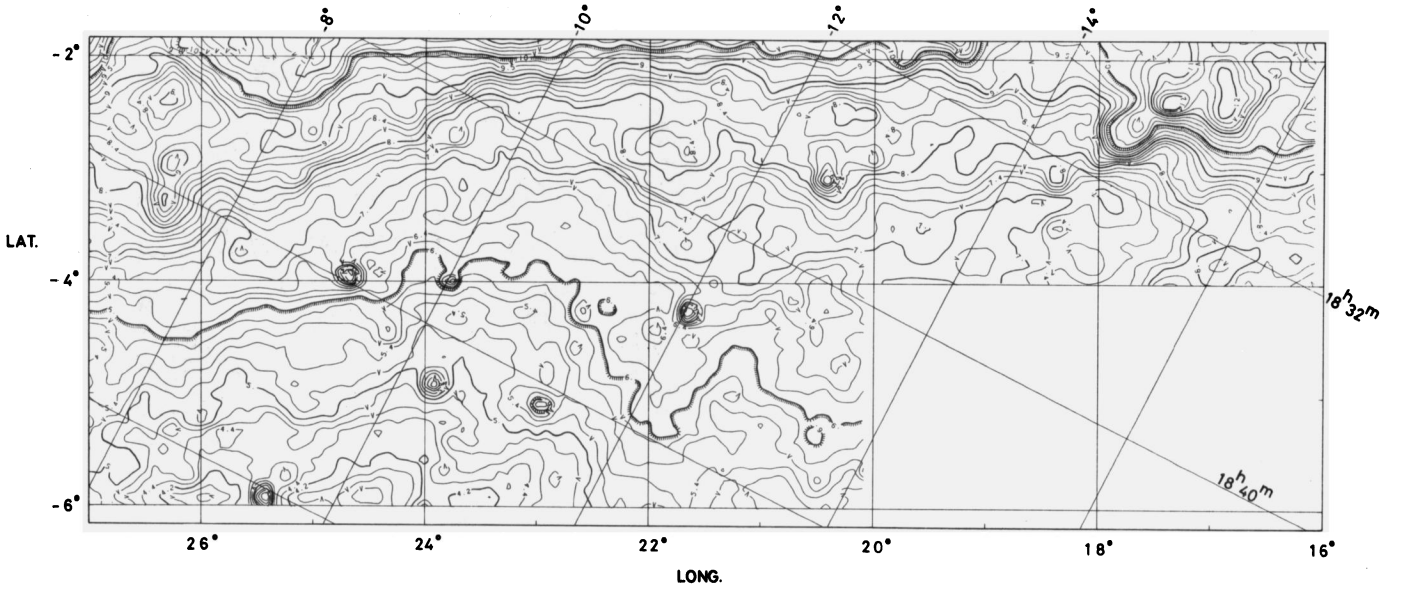


Figure 1f

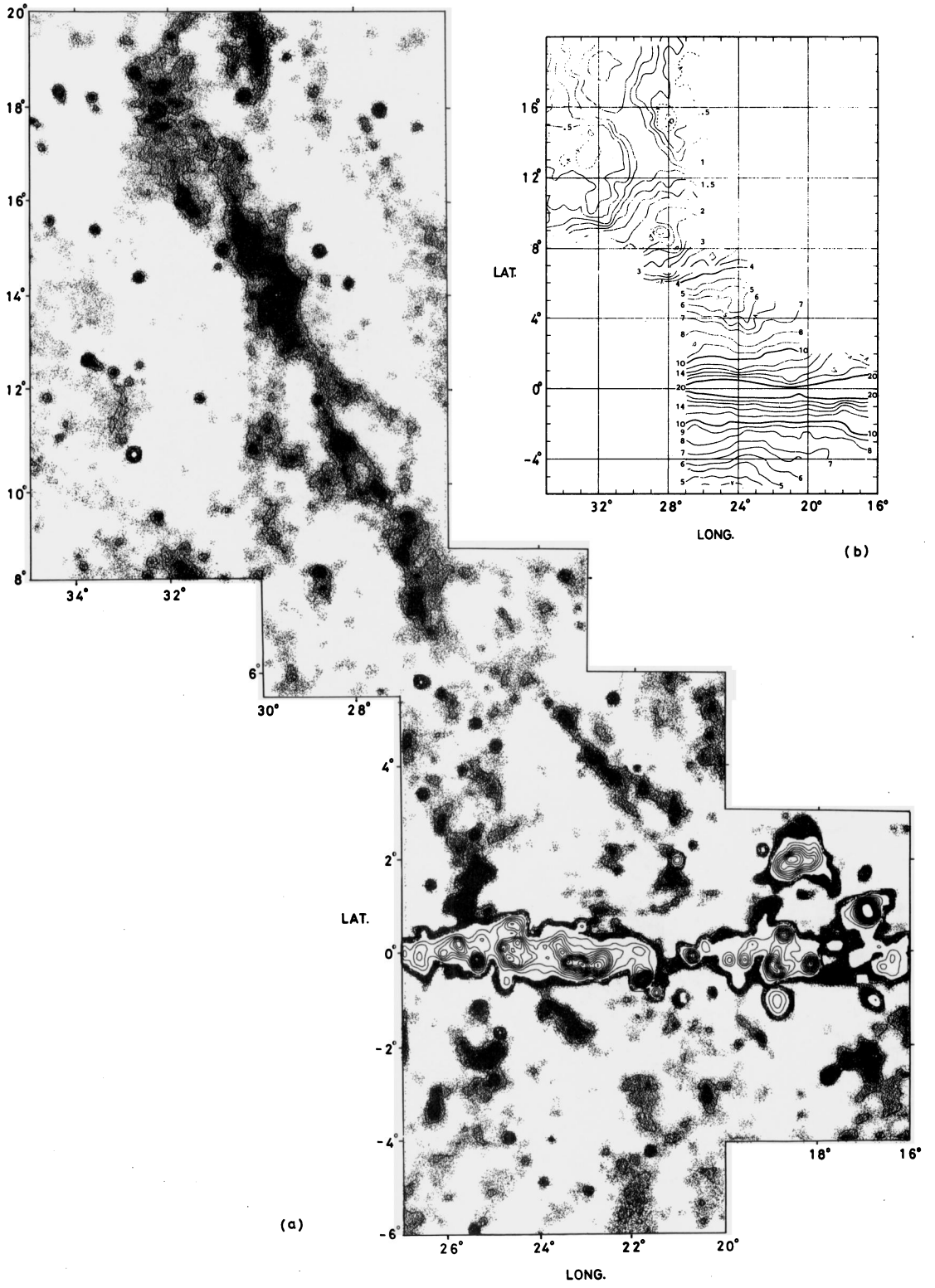


Figure 2 Grey-scale plot (a) of $\Delta T_b^1$ obtained after subtraction of the smooth background (b; top right) from the original $T_b$ distribution (see the text). Contour lines are superposed with intervals of 0.3 K from $\Delta T_b^1 = 0$ to 3 K and 3 K at $\Delta T_b^1 > 3$ K.

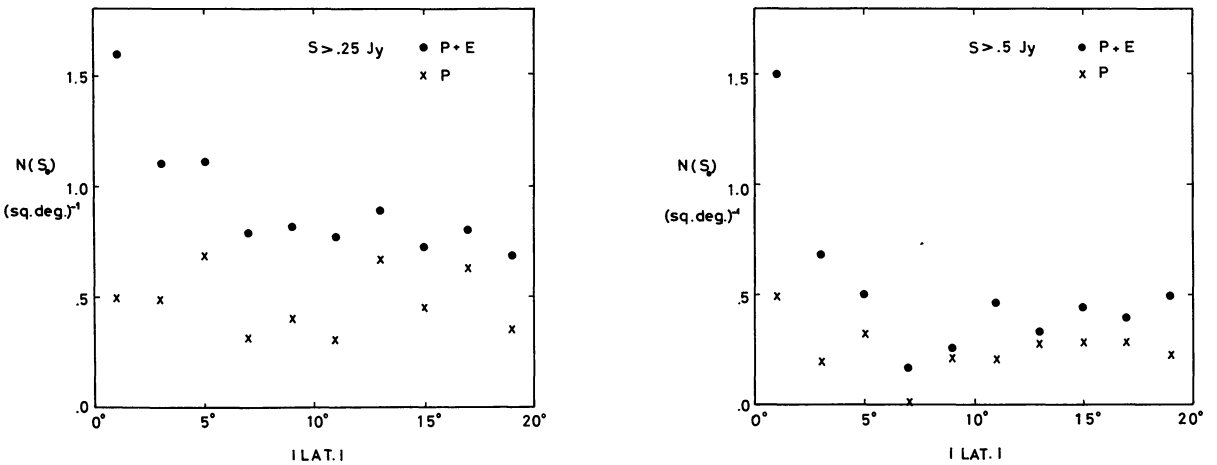


Figure 3 (a) Integrated counts $N(S_0)$ for radio sources listed in table 1 with the limiting flux density of $S_0=0.25$ Jy as a function of absolute value of galactic latitude. The open circles denote counts of all sources and the crosses counts of point sources only. (b) The same as a but for $S_0=0.5$ Jy.

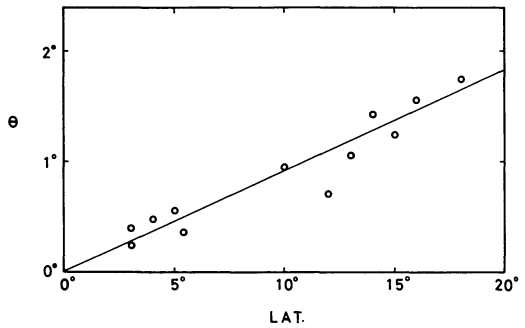


Figure 4 Half-width of the NPS ridge against galactic latitude. The width increases linearly with the latitude.

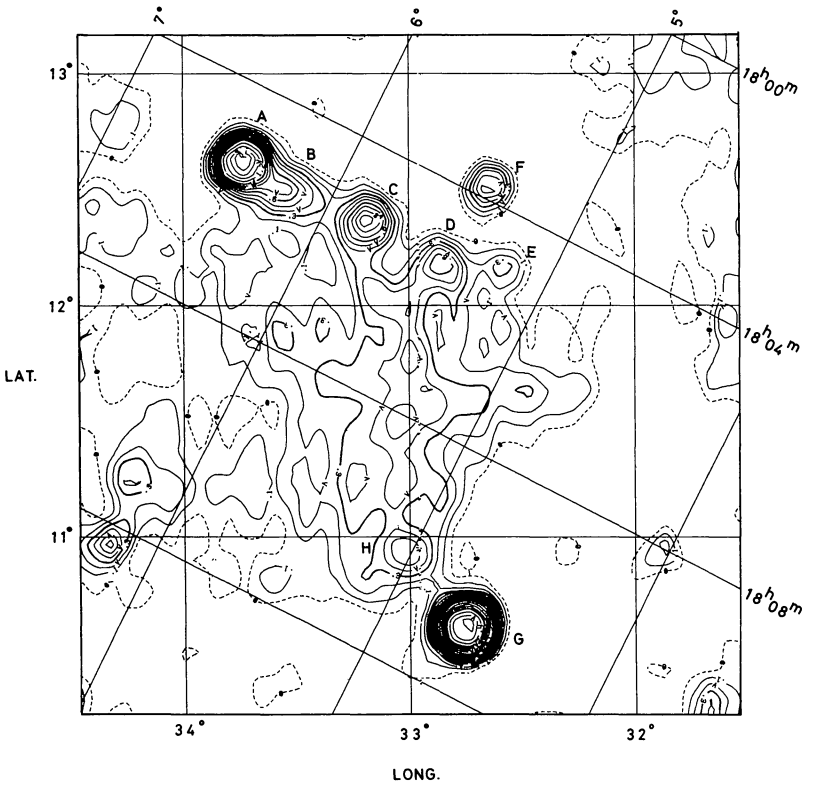


Figure 5 Contour plot of a small region around $(l, b)=(33°, 11.5°)$. The brightness temperature $T_b$ is indicated on each contour in deg. K. The four corners are set to zero. We find a peculiar chain of point sources within a thin strip of 5′ wide, 1.5° long (A–E). A diffuse bridge connects this chain-like association with the strong point source G (4C+04.63).